CORROSION BEHAVIOR OF POWDER METALLURGY ALUMINUM ALLOY 6061/AL_2O_3 METAL MATRIX COMPOSITES

Zuhair M. Gasem[1] and Amro M. Al-Qutub[1]

1: Assistant professor, Mechanical Engineering Department, KFUPM.
E-mail: zuhair@kfupm.edu.sa

ABSTRACT

The electrochemical behavior of aluminum alloy 6061/Al_2O_3 metal matrix composite was investigated in 3.5% NaCl aqueous solution. Two composite compositions were examined containing 10% and 30% (by volume) of sub-micron alumina particulates as the reinforcement phase. The composites were fabricated via powder metallurgy processing. Cyclic polarization tests were carried out to determine pitting potentials and repassivation potentials in deaerated 3.5% NaCl solution. The pitting potential was 50 mV more noble for the higher-content reinforcement composite, while the repassivation potentials were essentially identical. The scanning electron microscope was used to reveal pits morphologies generated potentiostatically at a potential 150 mV more noble than the open circuit potentials for two hours immersion in quiescent chloride solution. Excessive pitting of the matrix alloy was observed in both composites. Pits forming in the 6061/Al_2O_3/30p composite were more numerous and more uniformly dispersed compared to pits on the lower-content reinforcement composite which were deeper and more localized. Preliminary results suggest that pit initiation sites correlate with regions exhibiting agglomeration of the reinforcement particles.

Keywords: *6061 aluminum alloy, Corrosion, Aluminum metal matrix composite, Alumina reinforcement, Pitting.*

الملخص

يهدف هذا البحث إلى دراسة الخواص الكهروكيميائية لمواد مكون من الألمنيوم (٦٠٦١) كمحيط و حبيبات أكسيد الألمنيوم (Al_2O_3) كمقوي في محلول ملحي تركيز كلوريد الصوديوم فيه ٣,٥%. تمت دراسة مولفان يحتويان على ١٠% و ٣٠% بالحجم من حبيبات أكسيد الألمنيوم (مقاسها أصغر من ٧٥., ميكرومتر) منتجة بطريقة ميتالورجيا المساحيق. أستخدم الاستقطاب الترددي لقياس الجهد لبدأ التنقر وجهد عودة الخمود في محلول مفرغ من الهواء. وجد أن جهد التنقر للمواد الذي يحتوي على نسبة عالية من الطور المقوي أكثر إيجابية بمقدار ٥٠ mV ، بينما كان جهد عودة الخمود متساوياً للمولفين. أستخدم الماسح الطيفي لتقييم التنقر في كلا المولفين. وجد أن التنقر في حالة المواد عالي النسبة للطور المقوي ضحل ومنتشر بالتساوي مقارنة مع المواد الذي يحتوي على نسبة أقل من الطور المقوي الذي ظهر التنقر فيه أكثر عمقاً ومركز موضعياً. وقد أظهرالفحص الأولي المايكروسكوبي أن بداية التنقر قد تكون مرتبطة مع وجود تجمع حبيبات أكسيد الألمنيوم.

1. INTRODUCTION

Aluminum metal matrix composites (MMC) are being considered as good candidates for replacing conventional alloys in many industries such as aerospace, automotive, and sport due to their potential engineered properties. For example, continuous-fiber reinforced aluminum MMC are finding wide range of applications as structural composites using silicon carbide (SiC), graphite (Gr), alumina (Al_2O_3), and boron as reinforcements [Maruyama, 1999]. These composites offer high specific stiffness and strength compared to their matrix alloys. Discontinuous-fiber aluminum MMC, on the other hand, have been developed for applications concerned most with triboligical properties, thermal fatigue, and reduced coefficient of thermal expansion [Lloyd, 1994]. These composites consist mainly of whiskers, short fibers, and particulates of either SiC or Al_2O_3. Current and potential applications of discontinuous Al_2O_3 MMC have been used in lining of cylinder bores of cast aluminum engine blocks and in diesel-engine pistons [Kevorkijan, 1999]. The most extensively used aluminum matrix alloys include 2024, 6061, and 7075 heat treatable alloys.

Two main approaches are routinely employed for large-scale production of MMCs: the molten-metal process and powder metallurgy (PM) technique with the latter considered as more economical. The main advantage of the PM route is the reduced fabrication temperatures involved, which offer potentially better control of the reinforcement-metal interface. In the PM technique, powders of the matrix and the reinforcement phases are thoroughly mixed in the solid state, compacting to roughly 80% density, degassing, consolidated by vacuum hot pressing or hot isostatic pressure, followed by final hot pressing or hot extrusion. Significant amount of data is available regarding aluminum MMC and the correlations between processing parameters, microstructure, and mechanical properties [Lloyd, 1994]. Despite their improved mechanical properties, significant degradation can result in MMC due to environmental attack.

Potential constraints for widespread applications of these materials relate to their high production cost and to their increased corrosion susceptibility. The latter is related to the presence of microstructural heterogeneities which is an inherent characteristic of composites. In general, composites require combining of materials having considerable different corrosion behaviors leading to adverse effects on the corrosion resistance relative to their counterparts monolithic alloys. Several corrosion mechanisms are likely responsible for the reduced corrosion resistance of aluminum MMC compared to their parent alloys [Turnbull, 1992]: (i) galvanic coupling of the matrix and the more noble reinforcement, (ii) micro-crevice attack at the matrix-reinforcement interface, (iii) preferred localized attack at reactive intermetallics that form as a result of metal-reinforcement reactions during high temperature processing, (iv) structural flaws in the aluminum passive film near the interface, (v) and processing related defects such as porosity, poor homogeneity of reinforcement, residual stresses, and elemental segregation.

2. BRIEF REVIEW OF CORROSION MECHANISMS IN MMC'S

The galvanic coupling of aluminum with a noble reinforcement was proposed by many researchers as the main corrosion enhancement mechanism in Al/SiC, when exposed to chloride containing solutions [Hihara and Latanision, 1992; Nunes and Ramanathan, 1995]. Trazaskoma [Trzaskoma, 1990] and Ahmed [Ahmed et al., 2000] attributed enhanced pit initiation to increased precipitation of second-phase intermetallics in the vicinity Al/SiC interface. Aylor and Moran [Aylor and Moran, 1985] associated increased pitting corrosion in Al/SiC whiskers to crevices formed at the interface. Mansfeld and co-workers [Mansfeld et al., 1990] ascribed decreased corrosion resistance of Al/SiC particulate to crevices forming at the interfaces. Several other researchers proposed that alloy/ceramic interfaces are preferred sites for passive film breakdown leading to pits initiation. They hypothesized that film breakdown at the metal/ceramic interface is due to differences in the characteristics of passive films forming on different underlying materials [Aylor and Moran, 1985; Nunes and Ramanathan, 1995; Kruger et al., 1995].

Much of the early work on Al/Al_2O_3 MMCs focused on short and continuous fiber reinforcement types. The resistivity of high purity alumina (99.7% Al_2O_3) is greater than about 10^{14} Ω.cm [Bolz and Tuve, 1973], compared to 3.7 x 10^{-6} Ω.cm for annealed 6061 monolithic alloy, and therefore galvanic corrosion is unlikely for high purity alumina reinforcements. Formation of interphases between the metal alloy and the ceramic reinforcement during high temperature casting was observed without severe interfacial corrosion or interphases delamination [Champion et al., 1978; Metzeger et al., 1983]. Agrawala [Agrawala, 1982] reported preferential corrosion in the vicinity of an unspecified purity Al_2O_3 fiber in a 6061-T6 cast aluminum matrix exposed to 3.5% NaCl solution for 500 hours (whether the solution was aerated or deaerated was not stated). No investigation was made for the microstructural phases at the region of corrosion. Yang and Metzger [Yang and Metzger, 1981] tested the corrosion resistance of an experimental composites consisting of chopped Al_2O_3 fibers introduced into a stirred 50% solid slurry of Al-2%Mg alloy. Bonding was due to the formation of $MgAl_2O_4$ layer at the matrix/fiber interfaces. Accelerated immersion and polarization tests in NaCl solution containing H_2O_2 showed severe selective attack in the matrix adjacent to the fibers. Pits were attributed to rapid corrosion of Mg_2Al_3, which formed near the fiber due to Mg segregation during solidification.

Saxena et al. [Saxena et al., 1993] investigated the erosion-corrosion behavior of an aluminum alloy reinforced with 10% vol. alumina fibers. The composite exhibited increased susceptibility to pitting apparently owing to the presence of unidentified active phases near the matrix/fiber interfaces. Traverso and Beccaria [Traverso and Beccaria, 1998] examined the corrosion behavior of 6061/10% Al_2O_3 (approximately spherical with a medium size of 10 μm in diameter bonded by silicoaluminate phase to the matrix). Long exposure to seawater for 360 hr showed localized corrosion taking place at the matrix grain boundaries, supposedly due to Al_2Cu precipitation at grain boundaries. No evidence of localized corrosion occurring

at the matrix-alumina interfaces was shown. Monticelli et al. [Monticelli et al., 1995] studied the localized corrosion of aluminum/Al_2O_3 particulate and fiber composites MMCs (15% vol. fraction for both) in 0.1 M aerated NaCl at room temperature. The particulate MMC was produced by powder metallurgy followed by hot extrusion. No notable galvanic corrosion occurred at the interface in the Al_2O_3-particulate MMC. However, the Al_2O_3 fiber MMC showed detrimental localized corrosion behavior. Polarization curves indicated higher cathodic currents associated with fiber MMC as compared to particulate MMC. This behavior was related to residual stresses at the matrix/fiber interface which led to microcracks formation and subsequently flawed the passive film; hence increased corrosion current. Nunes and Ramanathan [Nunes and Ramanathan, 1995] investigated the aqueous corrosion behavior of Al/Al_2O_3 and Al/SiC MMCs with different particulate sizes and two volume fractions. The reinforcements were pretreated and added into the molten alloy, the mixture poured into copper mold, and allowed to solidify. The main observations were: (1) the number of pit initiation sites was significantly higher in the composites than in the alloys, (2) pits in the Al/SiC composite were deeper than those in Al_2O_3 based composite probably because SiC particles were more efficient cathodic sites, (3) micro-crevices and pits initiated preferentially at regions corresponding to phase discontinuities and second-phase particles, (4) the micro-crevice formation was more widespread in regions associated with clusters of Al_2O_3 particles, and (5) average corrosion weight loss for Al/Al_2O_3 composite after 28 days exposure demonstrated higher corrosion rates with increased Al_2O_3 size and volume fractions.

The research work cited above considered relatively large size Al_2O_3 particulate reinforcement (5-10 microns). There is not much published work related to sub-micron size particulate Al_2O_3 aluminum MMC and their effects on the corrosion resistance. Powder metallurgy is the preferred processing method for such composites. The objective of the present work is therefore to examine the corrosion behavior of sub-micron Al_2O_3 particulate aluminum alloy MMC in 3.5% NaCl.

3. EXPERIMENTAL

3.1 Composites

The composites examined in this study were fabricated by Frauhofer Institute Fetrigungstechnik Materialforschung, Germany, using powder metallurgy technique. Atomized 6061 aluminum alloy powder (nominal composition: 0.6% Si, 0.7% max Fe, 0.3% Cu, 1% Mg, balance Al) mechanically mixed in an inert environment with Al_2O_3 powder. Stearic acid was added to the powder blend to reduce particle clustering and may have reacted with the alloy forming approximately less than 1% oxide and carbide dispersoids. The milled powder was cold compacted, canned, degassed at 400 Cº for 8 hours, and evacuated. A final step of hot extrusion was performed at 550 Cº producing a 17 mm rod. Two different composite compositions were developed having volume fractions of 10% and 30%. The microstructure was examined metallographically.

3.2 Polarization Test

Specimens for corrosion testing were sliced out from the extruded 17 mm rod having between 2 to 3 mm in thickness. Specimens were ground to 600 grit, polished down to a surface roughness of 6 μm with diamond paste, rinsed vigorously in acetone, rinsed in distilled water, and directly inserted into a standard flat cell. The electrochemical tests consisted of open circuit potential (E_{oc}) monitoring, cyclic anodic polarization, and pontentiostatic holds. Polarization testing was carried out using a Princeton Applied Research (PAR) system model 273 linked to a PC and controlled by a commercial software. Specimens were mounted in the cell exposing approximately 1 cm^2 to the corrosive solution for more than 3 hrs to stabilize at E_{oc}. Scans started from –300 mV_{SCE} to an apex potential of 500 mV_{SCE} or an apex current of 1 mA, which ever reached first, at a constant scan rate of 1 mV/s. The corrosive solution was quiescent 3.5% NaCl prepared from distilled water at 23 Cº. Deaeration was performed by purging nitrogen gas through the electrolyte before and during the measurements. All potential measurements are reported versus SCE.

3.3 Pit Morphology

One specimen from each composite composition was held potentistatically at 150 mV more positive relative to E_{oc} for two hrs in quiescent 3.5% NaCl to stimulate pitting corrosion. Specimens were cleaned in nitric acid for few seconds to remove corrosion product. Thin layer of gold was applied to reduce charging. A scanning electron microscope was used at 15 KV to examine the pitting behavior and morphologies in both composites.

4. RESULTS

4.1 Microstructure

The microstructures of as polished 6061/Al_2O_3 containing 10% and 30% are shown in Figure 1. Etching in Keller's reagent did not reveal additional contrast. Alumina particulates appear darker than the aluminum matrix. Clustering of the sub-micron alumina reinforcements is pronounced in the lower volume fraction composite and can be described as islands surrounded by the matrix alloy with much more lower density of the reinforcement (Figure 1a). The reinforcements, on the other hand, appear homogeneously distributed in the 30% vol. fraction composite. This is may be attributed to different processing which was not documented by the manufacturer.

4.2 Corrosion Potentials

Open circuit potentials for these composites are summarized in Table 1 for aerated and deaerated conditions. E_{oc} values are essentially similar for both composites in the aerated solution. The E_{oc} for 6061/Al_2O_3/30p becomes more negative in the deaerated condition. This is may be due to different level in solution deaeration attained for each composite. It should be pointed out that Aylor and Moran [Aylor and Moran, 1985] reported a value of –720 mV vs. SCE for a monolithic powder metallurgy 6061 immersed in aerated ASTM ocean water.

4.3 Cyclic Polarizations

Figure 2 shows the cyclic polarization curves for both composites in deaerated 3.5% NaCl solution. These curves demonstrate that the pitting or breakdown potential (the potential above which pits are initiated, E_{bd}) for the higher reinforcement composite is slightly more noble by almost 50 mV while both composites show similar repassivation potential (E_{rp}), which is the potential below which pits repassivate. Assuming the difference in E_{oc} is genuine, the cathodic current for 6061/Al_2O_3/30p is consistently lower than 6061/Al_2O_3/10p composite. Figure 3 exhibits the cathodic polarization curves for the examined composites in aerated 3.5% NaCl. The anodic polarization curves for both composites showed continuous increase in corrosion current density indicating susceptibility to pitting and are not reported here. Similar to the behavior observed in the deaerated solution, the cathodic current is notably higher in the composite with the lower reinforcement content for the same potential.

4.4 Potentiostatic test

Figure 4 shows typical SEM micrographs for 6061/Al_2O_3/10% and 6061/Al_2O_3/30% immersed in aerated 3.5% NaCl and held at a potential of 150 mV more positive relative to the open circuit potential. The lower magnification micrographs illustrate the distribution of propagating pits whereas the higher magnification micrographs are intended to delineate pits morphologies. Comparing Figures 4a and 4c indicates higher pits density associated with the higher reinforcement composite. In addition, pits in the 6061/Al_2O_3/10p appear larger and deeper than in 6061/Al_2O_3/30p. Figure 4b exhibits a single propagating pit with no apparent other initiating pit sites in the surrounding area for 6061/Al_2O_3/10p. For identical testing condition and micrograph magnification, Figure 4d shows a number of propagating pits and numerous stable pits in 6061/Al_2O_3/30p.

5. DISCUSSION

Monolithic aluminum alloys and aluminum based MMC composites generally pit in solutions containing Cl^- ions. Fresh surfaces of aluminum alloys passivate rapidly when exposed to oxygen containing environments forming surface oxide films which are poor conductors for charge transfer. This restricts the cathodic areas to localized regions on the film which contain flaws such as phase discontinuities, second-phase precipitates, reinforcements, impurities, and microporosities [Thompson and Wood, 1978; Thompson 1982]. Residual stresses in the matrix adjoining the reinforcement (arising mainly due to differences in the coefficient of thermal expansion) are preferred sites for dissolution and pitting [Nunes and Ramanathan, 1995].

Pitting corrosion proceeds by initiation and propagation of pits. Pits initiation start with the adsorption of Cl^- ions at the film flaws, followed by chemical reactions between the Cl^- ions and the oxide film resulting in a localized damage of the film [Foley, 1986]. At each initiated pit site, a high local anodic current density is realized with a decreased oxygen concentration

due to limited oxygen transport in the pit. Hydrolysis of metal cations encourages Cl^- ion migration to maintain charge neutrality and decreases the pH inside the occluded pit. High chloride ion contents and low pH environments tend to accelerate the anodic dissolution reaction within the pit leading to stable pit propagation stage [Aylor and Moran, 1985].

In MMCs, surface variations due to the presence of ceramic reinforcements in the matrix could also promote film flaws and hence increased pitting [Trzaskoma, 1983; Kolman and Butt, 1997]. Therefore, it is proposed here that alumina particulate clusters are the preferred sites for pit initiation in 6061/Al_2O_3 exposed to 3.5% NaCl. The presence of a very large number of reinforcement clusters at the surface of 6061/Al_2O_3/30p, as evident from Figure 1b, led to uniform distribution of pitting in the matrix as can be seen in Figure 4c and 4d. In the lower reinforcement composite, however, alumina clusters are farther apart as evident in Figure 1a and, therefore, the pits density is lower. This is consistent with Figure 4a. In addition, the growing pits tend to cathodically protect smaller pits and this might explain the numerous non-propagating pits surrounding the growing ones.

The difference in cathodic current densities is not well understood at present. A possible reason may be attributed to experimental error associated with aerated cathodic polarization for the 6061/Al_2O_3/30p and different deaeration level for polarization curves in deaerated tests. However, the same behavior is observed in the aerated solutions which might suggest that the difference could be genuine. Further tests need to be undertaken to investigate this behavior.

6. CONCLUSIONS

The corrosion behavior of 6061/Al_2O_3 composites with two volume fractions of the reinforcement were examined in 3.5% NaCl. The preliminary conclusions of this research:

1. Sub-micron alumina reinforcement agglomerate and form clusters which were observed in both composites examined, with increased spacing between clusters for the lower volume fraction composite.
2. The number of pit initiation sites appears to increase with the volume fraction of the reinforcement.
3. Pits in the 6061/Al_2O_3/30p composite were more numerous and shallow than in 6061/Al_2O_3/10p when polarized in quiescent 3.5% NaCl solution.
4. Increasing the reinforcement volume fraction did not alter E_{oc} considerably in aerated condition.
5. The current density in aerated solution increased rapidly as the potential increased anodically implying low pitting resistance of these composites.
6. In deaerated solution, the repassivation potential was independent of the volume fraction of the reinforcement. However, increasing the reinforcement fraction delayed pitting to a more noble value.

7. REFERENCES

1. Agrawala, V.S., 1982, Extended Abstracts, Vol. 82-1, Abstract No. 15., The Electrochemical Society, Montreal, Canada.
2. Ahmed, Z., Paulette, P.T., and Aleem, B.J.A., 2000, *Journal of Materials Science*, 35 (10), pp. 2573-2579.
3. Aylor, D. M. and Moran, P.J., 1985, *Journal of Electrochemical Society*, 130 (6), pp 1277-1281.
4. Bolz, R.E., and Tuve, G.L., 1973, CRC Handbook of Tables for Applied Engineering Science, 2nd Ed., CRC press, p. 262.
5. Champion, A.R., Kruger, W.H., Hartmann, H.S., and Dhingra, A.K.,1978, *Proceedings of the International Conference on Composites of Materials,* p. 883, The Metallurgical Society of AIME Toronto, Canada.
6. Foley, R.T., 1986, *Corrosion*, 42 (6), pp 277-284.
7. Hihara, L.H. and Latanision, R.M., 1992, *Corrosion*, 48 (7), pp 546-552.
8. Kevorkijan, V.M., 1999, *Advanced Materials and Processes*, 155 (5) pp 27-29.
9. Kolman, D.G., and Butt, D.P., 1997, *Journal of Electrochemical Society*, 130 (11), pp 3785-3791.
10. Kruger, J., Lillard, R.S., Streinz C.C., and Moran, P.J., 1995, *Materials Science and Engineering*, A198 (11), pp 132-138.
11. Lloyd, D.J., 1994, *International Materials Review*, 39 (1), pp 1-23.
12. Mansfeld, F., Lin S., Kim, S., and Shih H., 1990, *Journal of Electrochemical Society*, 137 (1), pp. 78-82.
13. Maruyama, B., 1999, *Advanced Materials and Processes*, 155 (6), pp 47-52.
14. Metzger, M. and Fishman S.G., 1983, *Industrial and Engineering Chemistry: Product Research and Development*, vol. 22, pp 296-302.
15. Monticelli, C., Zucchi, F., Bonollo, F., Brunor, G., Frignani, A., and Trabanelli, G., 1995, *Journal of Electrochemical Society*, 142 (2), pp 405-410.
16. Nunes, R.C.R. and Ramanathan L.V., 1995, *Corrosion*, 51(8), pp 610-617.
17. Saxena, M., Modi, O.P., Prasad, B.K., and Jha, A.K., 1993, *Wear*, vol. 169, pp 119-124.
18. Thompson G.E., and G. C. Wood, 1978, *Corrosion Science*, vol. 18, pp 721-728.
19. Thompson G.E., P.E. Doherty, and G. C. Wood, 1982, *Journal of Electrochemical Society*, vol. 129, 1982, pp 1515-1521.
20. Traverso, P. and Beccaria, A.M., 1998, *Surface and Interface Analysis*, vol. 26, pp 524-530.
21. Trzaskoma P.P., 1990, *Corrosion*, 46 (5), pp 402-407.
22. Trzaskoma P.P., E.M. McCaffery, and C.R. Crowe, 1983, *Journal of Electrochemical Society*, vol. 130, pp 1804-1810.
23. Turnbull, A., 1992, *British Corrosion Journal*, 27 (1), pp 27-35.
24. Yang, J.Y. and Metzger, M., 1981, Extended Abstracts, Vol. 81-2, Abstract No. 155, The Electrochemical Society, Denver, Colorado.

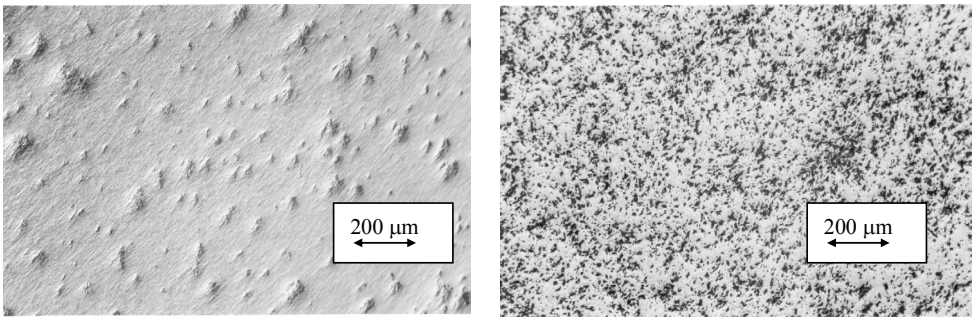

(a) **(b)**

Figure 1: Optical micrographs for as polished 6061/Al_2O_3p with particulate volume fraction: (a) 10% and (b) 30%. Alumina particulates appear darker than the matrix alloy.

Table 1: Average corrosion potentials for 6061/Al_2O_3p immersed in aerated and deaerated 3.5% NaCl for 3 hours.

Composite	Aerated E_{oc} (mV vs. SCE)	Deaerated E_{oc} (mV vs. SCE)
6061/Al_2O_3p/10%	-745	-1080
6061/Al_2O_3p/30%	-750	-1310

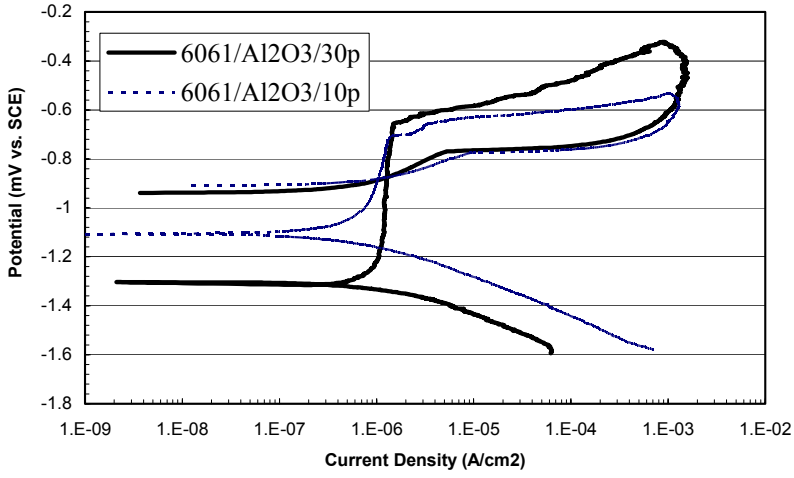

Figure 2: Cyclic polarization of powder metallurgy 6061/Al_2O_3 MMC immersed in deaerated 3.5%NaCl.

Top

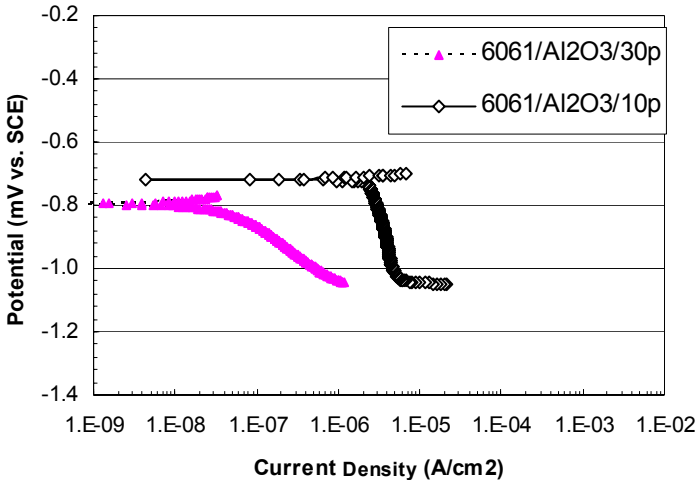

Figure 3: Cathodic potentiodynamic polarization of powder metallurgy 6061/Al_2O_3 MMCs immersed in aerated 3.5%NaCl.

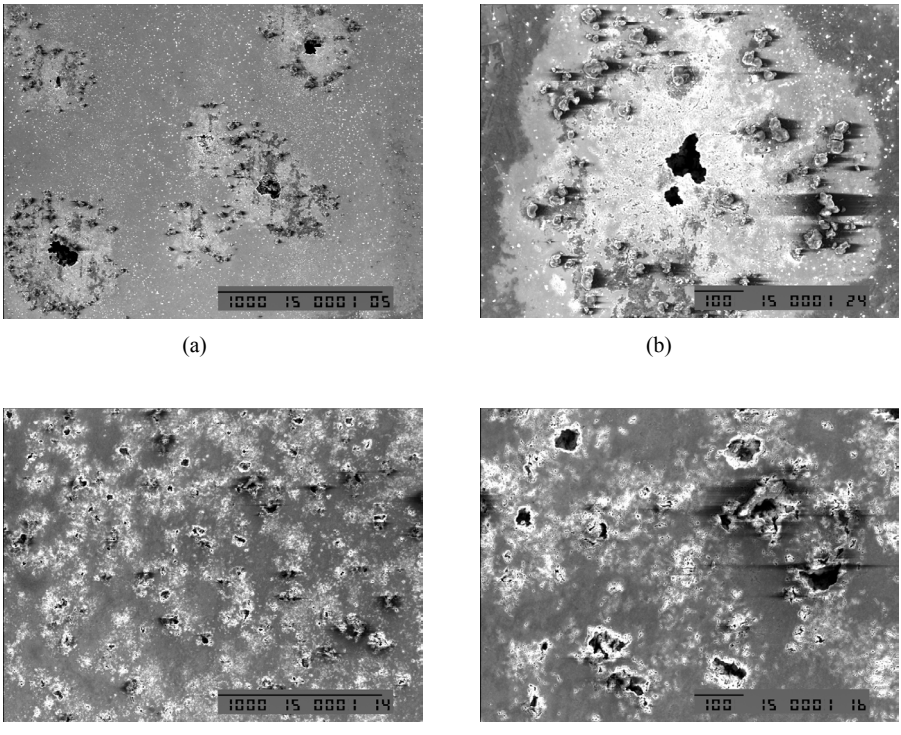

(a) (b)

(c) (d)

Figure 4: SEM micrographs showing pits morphologies of 6061/Al_2O_3 MMC after potentiostatic polarizing at 150 mV vs. E_{oc} for two hours in aerated 3.5% NaCl; (a) 6061/Al_2O_3/10p at X50, (b) 6061/Al_2O_3/10p at X150, (c) 6061/Al_2O_3/30p at X50, and (d) 6061/Al_2O_3/30p at X150.

Top